BEAM–BASED TRAJECTORY ALIGNMENT IN THE NISUS WIGGLER

H. Loos*, T. V. Shaftan, L. F. DiMauro, A. Doyuran, W. S. Graves, E. D. Johnson, S. Krinsky,
J. Rakowsky, J. Rose, B. Sheehy, J. Skaritka, J. Wu, L.–H. Yu, Y. Zhao,
BNL–NSLS, Upton, NY 11973, USA

Abstract

The Deep Ultra Violet FEL is under commissioning in the Source Development Laboratory (SDL) at NSLS. The goal of the experiment's first stage is to obtain 400 nm SASE. The magnetic system of the FEL includes the 10 m long NISUS wiggler with 3.9 cm period. Deviations from the design trajectory should be less than 60 μm within one gain length. In this paper we describe the hardware and methods of trajectory control and alignment used for this experiment. Measurements of the actual beam trajectory, its correction, and a method to obtain the dipole field errors from trajectory measurements are presented.

1 INTRODUCTION

The Source Development Laboratory at the NSLS operates a normal conducting accelerator with a laser driven RF gun to provide a high brightness electron beam [1] suitable for various FEL experiments with the NISUS wiggler as the radiator. For the different stages in the scientific program from SASE at 400 nm to HGHG [2] at 200 nm fundamental and 66 nm 3rd harmonic wavelength the requirements on electron beam trajectory straightness and beam size matching are more and more demanding. Here we describe the NISUS wiggler layout [3] with its tools for trajectory control, the diagnostic elements for trajectory and beam size measurement, and the methods employed to obtain the desired trajectory and matching.

2 NISUS UNDULATOR

The NISUS undulator is a permanent magnet hybrid structure with its parameters given in Table 1. Whereas the wiggler structure [4] itself provides natural focusing in the vertical direction, the focusing in the horizontal direction is done by regions of canted poles along the wiggler giving quadrupole focusing horizontally and defocusing vertically in each of the 16 sections of the whole wiggler. The peak focusing strength of the canted pole region in the undulator can be described by a modified Halbach formula [4]

$$\frac{dB}{dx} = 2\theta B_0 \left(\frac{5.47}{\lambda_W} - 3.6 \frac{g}{\lambda_W^2} \right) \qquad (1)$$

which gives a result that is in good agreement with the measured value. Additional magnetic fields can be superimposed on the static magnetic undulator field by means of a so–called 4–wire structure in every section consisting of 4 independently powered wires, which allows for any combination of vertical and horizontal dipole as well as normal and skew quadrupole fields. These coils are integrated within the vacuum chamber for the electron beam. Their main purpose is to obtain equal focusing strength at different electron beam energies and to correct vertical trajectory errors. Horizontal correction is provided by so called pancake coils which are located outside the main magnetic structure of the wiggler and have a rather uniform dipole field within the gap.

Table 1: NISUS undulator parameters. 3rd column refers to STI–report [4], 4th column to BBA measurements.

Undulator			
Periods		256	
Sections		16	
Period length λ_W	mm	38.9	
Length	m	10	
Gap g	mm	20.6	
Peak field B_0	mT	310.4	296.4±0.6
Canted poles			
Periods/section		3	
Cant angle θ	mrad	0.108	
Gradient $C_{\rm CP}$	mT/m	103.1	108.9±1
4–wires			
Gradient $C_{\rm 4W}$	mT/A/m	7.18	7.12±0.08
Pancakes			
Dipole strength	μTm/A	35	

3 TRAJECTORY MEASUREMENTS

Along the NISUS wiggler are 16 retractable YAG monitors each with a periscope and image relay to an attached CCD camera. An automated procedure of the control system for the linac allows the consecutive measurement of centroid and beam size at each monitor within 2 minutes. Two additional monitors 1 m and 6 cm in front of the wiggler are included to record the initial conditions of the electron beam with respect to the wiggler. A green HeNe laser beam, aligned to apertures before and after the wiggler, provides a reference position for each monitor. The monitors are calibrated individually with a resolution of approximately 10 μm/pixel. The reproducibility of the trajectory measurements is 20 μm (rms), which is much smaller than the requirement for the first SASE experiment at 400 nm.

In order to apply a beam based alignment (BBA) scheme to the initial conditions of the electron beam in position and Twiss parameters at the NISUS entrance, a precise knowledge of the betatron wavelength for different energies and 4–wire focusing is necessary, since the wavelength cannot

* loos@bnl.gov

be obtained by a single trajectory measurement.

The quadrupole fields of the canted poles and the 4–wire coils cover only a part of each section. The betatron wavelength is much longer than a section length, so that it is valid to treat them as uniformly distributed along the undulator. Thus, the NISUS model is that of a long quadrupole with horizontal and vertical focusing given by

$$\begin{aligned} k_x^2\, B\rho &= C_{\rm CP} - C_{\rm 4W}\, I_{\rm 4W} \\ k_y^2\, B\rho &= -C_{\rm CP} + C_{\rm 4W}\, I_{\rm 4W} + \frac{B_0^2}{2\, B\rho} \end{aligned} \qquad (2)$$

with the parameters $C_{\rm CP}$ and $C_{\rm 4W}$ as the canted poles and 4–wire calibrations and B_0 as the wiggler peak field. From Eq. 5, discussed below, it is clear that varying the initial conditions (angle, position) of the electron beam while holding the beam energy and corrector fields constant, results in a pure sinusoidal modulation of the trajectory as a function of the distance along the undulator.

A nonlinear least squares fit algorithm was applied to some 80 trajectories and the resulting focusing strengths are shown in Fig. 1. The free parameters of Eq. 2 can now

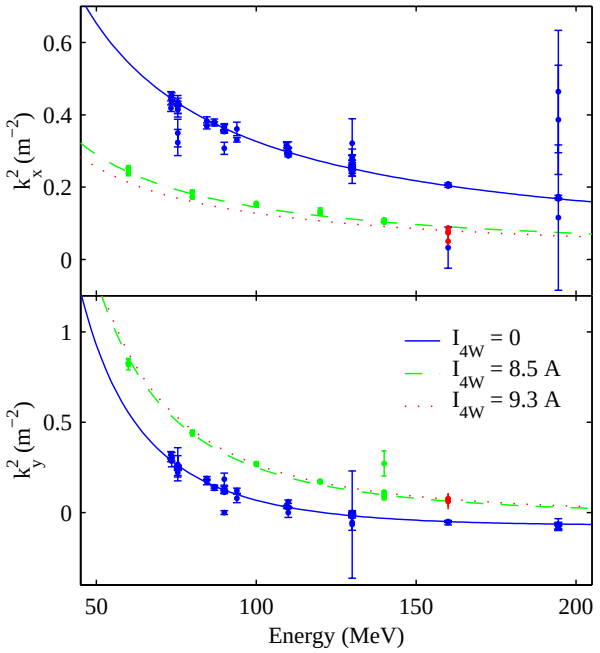

Figure 1: Horizontal and vertical focusing strength of NISUS for various energies and three different 4–wire currents.

be determined by a linear least squares fit and can be found in the last column of table 1. The peak field B_0 obtained from measurements of the radiation wavelength is consistent with the fit.

An automated correction of the position and angle of the electron beam at the NISUS entrance is obtained by measuring amplitude and phase of the betatron motion of the beam in NISUS and applying proper correction to two upstream trim correctors.

4 BEAM SIZE MEASUREMENTS

Of even more importance for SASE performance than the trajectory of the electron beam in NISUS is an accurate matching of the initial Twiss parameters.

4.1 *Emittance Measurement*

These parameters are obtained by an extension of the three screen method of emittance measurement [5] to the 16 (currently 13) monitors within NISUS. The result of such a measurement is shown in Fig. 2 for an unmatched electron beam. The measured Twiss parameters are then back transported to the last triplet before NISUS. The emittance and the calculated beam size at this position are in good agreement with this parameters obtained by a quad scan with this triplet.

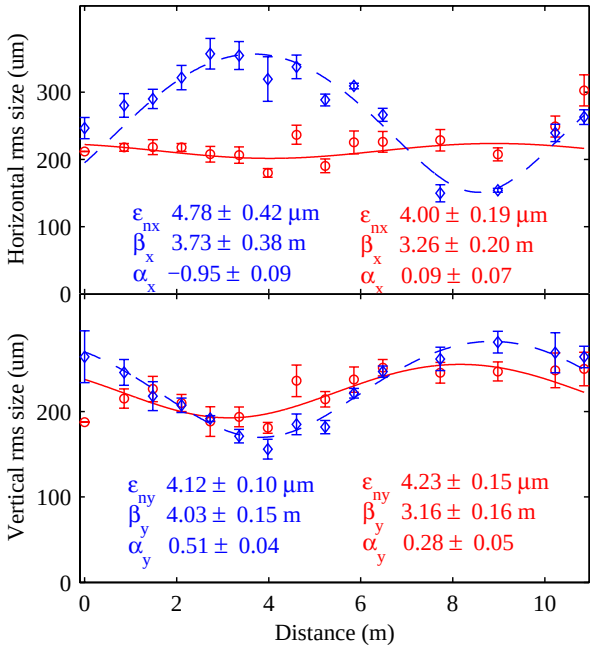

Figure 2: Horizontal and vertical beam size along the wiggler with electron beam parameters at NISUS entrance before (dashed) and after (solid) matching procedure.

4.2 *NISUS Matching*

With the known beam parameters at the last triplet before NISUS, better settings for this triplet can be calculated to match the beam in NISUS. These settings can be automatically sent from the measurement program to the linac control system to apply the correction. The result of such a correction step is shown in Fig. 2 with the matching considerably improved. An optimal matching could not be expected, because only one triplet was changed. Using additional quadrupoles in the future will give even better results.

5 NISUS FIELD ERRORS

Despite of precise magnetic field measurements and shimming procedures prior to the commissioning of the DUVFEL experiment, a large horizontal dipole field error and smaller horizontal and vertical kicks in NISUS were observed, when the first trajectory measurements were initiated. In order to better understand the nature of these errors and to develop a reliable method to properly correct them with the different corrector coils in NISUS, a method of measuring these field errors with the electron beam itself is discussed here.

5.1 Model with Field Errors

The model assumed constant focusing properties $k_{x,y}$ and a varying dipole field $B(z)$ along the wiggler. The differential equation for the horizontal movement x of a single particle and also the beam centroid is

$$x'' + k^2 x = \frac{B(z)}{B\rho}. \tag{3}$$

This equation can be solved generally:

$$x = x_0 \cos kz + \frac{x_0'}{k} \sin kz + \int_{z_0}^{z} d\alpha \frac{B(\alpha)}{k\,B\rho} \sin k\,(z-\alpha) \tag{4}$$

One can assume an average field error B_n in each section and carry out the integration section–wise under the condition that $2/3\ \Delta z\, dB/dz \ll B_0$. This means that the field variation dB/dz in a section length Δz must be much smaller than the peak field B_0. This is confirmed by magnetic measurements even in the extreme case of the field error being located over only one period. The individual beam positions x_n on each monitor can now be calculated as

$$x_n = x_{\mathrm{off},n} + x_0 \cos kz_n + \frac{x_0'}{k} \sin kz_n + \frac{1}{k^2 B\rho} \times$$

$$\times \sum_{j=1}^{n} B_n \left[\cos k\,(z_n - z_j) - \cos k\,(z_n - z_{j-1})\right]. \tag{5}$$

Offsets $x_{\mathrm{off},n}$ for the monitors have been included, because the monitors are not aligned with respect to the magnetic axis. Assuming a focal strength of the wiggler according to the model discussed above, this represents a system of linear equations for the trajectories which can be solved for the unknown parameters when measuring trajectories at different energies. One restriction on the parameters has to be imposed. Since any linear content of the field errors can be removed by a linear transformation of the variable x_n, either the magnetic center of the undulator has to be defined or the field errors have to be constrained to not contain any linear contribution.

5.2 Simulation of Field Error Measurement

In order to estimate the required precision of the trajectory measurement and the achievable precision of the calculated field errors, a simulation of this field error measurement is discussed here. The assumed field errors have a quadratic trend and are shown in the lower part of Fig. 3. The simulated trajectories for four different energies are in the upper part together with the fit to the model. A random

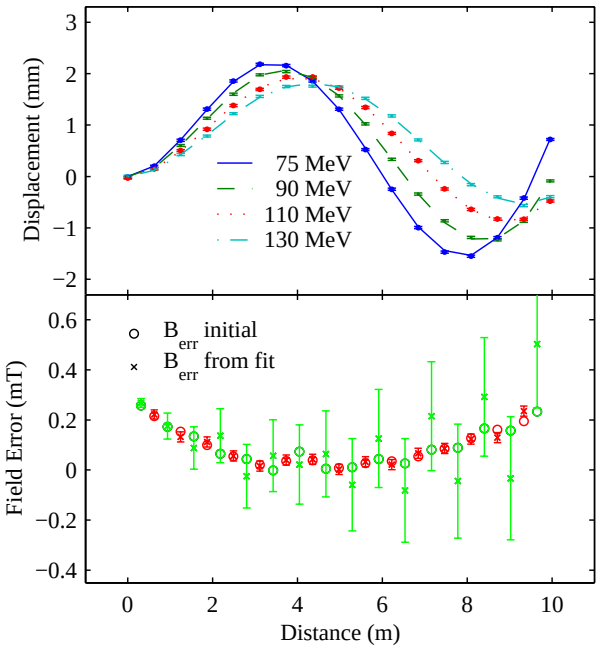

Figure 3: Simulation of dipole field error measurement. Lower part shows initial and calculated field error, upper part shows the simulated electron beam trajectories.

position error of $\Delta x = 30\,\mu m$ (rms) was added to the trajectories. The obtained field errors from this fit are shown in the lower part (green) and one can see unreliable large standard deviations ΔB of the field errors. They can be estimated by

$$\Delta B = \frac{2B\rho\,\Delta x}{\Delta z^2} \tag{6}$$

with section length Δz. The errors are highly correlated, as it turns out when the average dipole field errors over two sections (shown in red) are calculated. They reproduce very reliably the initially assumed errors.

6 REFERENCES

[1] W. S. Graves, et al., "Measured Properties of the DUVFEL High Brightness, Ultrashort Electron Beam", PAC 2001, Chicago, June 2001.

[2] L.–H. Yu, et al., "The DUV–FEL Development Program", PAC 2001, Chicago, June 2001.

[3] D. C. Quimby, et al., "Development of a 10–Meter Wedged–Pole Undulator", NIM A **285**, 281 (1989).

[4] Final report, "Magnetic Field Mapping of the NISUS Undulator", STI Optronics, Inc., March 2000.

[5] C. Bovet, "Comparison of Different Methods for Transverse Emittance Measurements and Recent Results from LEP", DIPAC 97, Frascati, 1997.